JOURNAL OF CATALYSIS **161,** 614–625 (1996)
ARTICLE NO. 0224

Reactivity of Pd/Al_2O_3, Pd/La_2O_3–Al_2O_3 and $Pd/LaAlO_3$ Catalysts for the Reduction of NO by CO: CO and NO Adsorption

M. Valden,*[,1] R. L. Keiski,† N. Xiang,* J. Pere,* J. Aaltonen,* M. Pessa,* T. Maunula,‡ A. Savimäki,‡ A. Lahti,‡ and M. Härkönen‡

*Department of Physics, Tampere University of Technology, P.O. Box 692, FIN-33101 Tampere, Finland; †Department of Process Engineering, University of Oulu, P.O. Box 444, FIN-90571, Oulu, Finland; and ‡Kemira Metalkat Oy, Catalyst Research, P.O. Box 171, FIN-90101 Oulu, Finland

Received July 31, 1995; revised March 4, 1996; accepted March 30, 1996

Industrially manufactured Pd catalysts supported on Al_2O_3, La_2O_3–Al_2O_3, and $LaAlO_3$ were prepared to contain different amounts of PdO. The effect of the chemical state of Pd on adsorption and thermal properties of CO and NO were investigated by temperature-programmed desorption (TPD) and Fourier transform infrared spectroscopy (FT–IR). CO adsorbed molecularly on all Pd catalysts forming linear and bridged CO species. The presence of PdO was found to strongly decrease the CO binding energy on Al_3O_3-supported Pd catalysts, as indicated by the subsequent lowering of the temperature of the TPD peak maximum. The destabilization of CO bonding was even further enhanced on Pd catalysts supported on $LaAlO_3$ and La_2O_3–Al_2O_3. The interaction of CO with the Al_2O_3, La_2O_3–Al_2O_3, and $LaAlO_3$ supports was negligible. In contrast to the behavior of CO, NO was observed to adsorb molecularly on Al_2O_3, La_2O_3–Al_2O_3, and $LaAlO_3$ supports with high efficiency. Strong absorption bands of NO in the range of 1600–1200 cm^{-1} were detected. The dissociation of NO, followed by the formation of N_2 and N_2O during the temperature programmed reaction, was seen on all the Pd catalysts. The importance of the chemical state of Pd and the La-induced effects on the reactivity of CO and NO are discussed.

1. INTRODUCTION

Nearly all catalytic surface reactions of technological relevance proceed under conditions where the simultaneous existence of a multi-component adsorbate system of various surface species, such as reactants, products, intermediates, and surface modifiers, is unavoidable. Despite this complexity, application of surface science methods to studies related to simple model systems has provided essential information to understanding the surface physics and chemistry occurring on real-world catalysts. The work reported here is a part of our ongoing surface reactivity studies of CO, NO, and O_2 on industrially manufactured, supported noble metal catalysts. The present paper illustrates the effects of surface modifications by oxygen and lanthanum on the surface chemistry of CO and NO adsorption on Pd catalysts.

Catalytic properties of palladium have received increasing attention because of their potential use in automotive emission control. Under certain reaction conditions, a Pd-only catalyst has been found to be as effective as an ordinary three-way catalyst for the simultaneous removal of NO, CO, and hydrocarbons (1, 2). However, the Pd-only catalyst has a poor NO reduction efficiency compared to Rh, especially in an oxygen-rich environment. Attempts to improve the catalytic performance of Pd have been made by placing it in contact with various base metal oxides and rare earth oxides (3).

Despite the fact that the use of Pd in automotive exhaust catalysis is increasing, rather little is known about the surface complex formation during the catalysis. This is due to several possible oxidation stages of Pd in transient exhaust gas conditions. Recently, results of FT–IR studies on NO and CO adsorption on Pd catalysts have been reported indicating the complexity of the NO and CO adsorption phenomena (4–14).

The present study focuses on the adsorption and decomposition of CO and NO on Pd catalysts with different oxidation stages and washcoat structures by using different surface science methods. The chemical state of the catalyst was examined by XPS (X-ray photoelectron spectroscopy). The type and strength of surface bonding were detected by separate FT–IR and TPD analyses. The aim was to determine the importance of the chemical state of Pd and the presence of La promoters for the CO and NO bonding on active sites, both on the noble metal and on acid sites in the washcoat.

2. EXPERIMENTAL

TPD (temperature programmed desorption) experiments were carried out in a multi-technique UHV chamber with a base pressure less than 5×10^{-11} Torr (1 Torr

[1] Author to whom correspondence should be addressed. Fax: +358 31 316 2600; E-mail: valden@ee.tut.fi.

0021-9517/96 $18.00

TABLE 1

Structural Properties of Pd Catalysts (17)

	Pd/Al_2O_3 (A)	Pd/Al_2O_3 (B)	Pd/Al_2O_3 (C)	$Pd/LaAlO_3$	Pd/La_2O_3–Al_2O_3
Finishing T of the heat treatment (K)	1223	No treatment	773	1223	1223
BET surface area ($m^2\ g^{-1}$)	116	155	117	5.9	50
Pore volume ($cm^3\ g^{-1}$)	0.38	0.33	0.35	0.05	0.20
Mean pore radius (nm)	6.6	4.2	6.0	17	8
Pd loading (wt%)	7.6	1.9	7.6	8.0	7.2
Pd dispersion (%)	2.2	27	1.2	1.2	2.0
Pd particle diameter (nm)	51	4.2	95	96	55
Chemical state, PdO (%)	10	40	90	75	90

$= 133.3\ N\ m^{-2}$). The UHV chamber is equipped with a molecular beam generation system and a quadrupole mass spectrometer (Balzers QMG 420) for molecular beam-scattering studies as well as other surface characterization techniques such as LEED/AES (low energy electron diffraction/Auger electron spectroscopy, Fisons RVL 900) and XPS (VG ADES-400). The molecular beam scattering system provides a high intensity molecular beam which has a flux of $6.25 \times 10^{13} \pm 5.0 \times 10^{12}$ molecules $cm^{-2}\ s^{-1}$ and a beam diameter of 5.5 mm at the position of the sample. The apparatus used in this work has been described in detail elsewhere (15).

The supported Pd catalysts used in this work were supplied by Kemira Metalkat Oy (Finland). A flat metal foil was coated with the washcoat, thus allowing the analysis of a real exhaust catalyst. The washcoat layer on the metal substrate comprised Al_2O_3, La_2O_3–Al_2O_3, or $LaAlO_3$. The noble metal loading of Pd on the washcoat was in the range of 7.2 to 8.0%, except Pd/Al_2O_3 (B) for which the Pd loading was 1.9%. The samples were first reduced using the following sequence: $N_2 \rightarrow 673\ K \rightarrow 673\ K$ for 2 h in $H_2 \rightarrow 673\ K \rightarrow 323\ K$ in N_2 after which they were treated cyclically in air at temperatures 773 K (2 h) to 1223 K (2 h) for a total period of 12 h. The finishing temperature of the cyclic treatment was a variable to evaluate the final chemical state of palladium. The specific surface areas (BET) and noble metal dispersions were calculated by using adsorption isotherms of nitrogen at 77 K and CO at 298 K, respectively.

The amount of PdO was determined by XPS. A Kratos XSAM 800 photoelectron spectrometer was employed for XPS measurements using Mg$K\alpha$ radiation (1253.6 eV). Two chemical states of Pd were distinguishable from the XPS results. This was evident by the relatively high FWHM's of the Pd $3d_{5/2}$ spectra ranging from 1.8 eV to 2.2 eV and was further verified by a peak-fit analysis. The deconvoluted peak envelopes revealed two distinct chemical states of palladium. The binding energies were centered at 335.4 eV and 336.7 eV. These energies can be assigned to the corresponding binding energies of metallic Pd and oxidized Pd (PdO) (16). The percentage of PdO was then calculated from the integrated peak areas. The details of the preparation and characterization of the supported Pd catalysts have been described in Ref. (17). The structural properties of the catalysts and the XPS results concerning the chemical states of Pd are summarized in Table 1.

The only impurity observed in the XPS analysis was carbon, the concentration of which remained at a constant level during the experiments. Since it was impossible to deduce whether carbon was associated with the support alone or whether it was associated with Pd particles, it was assumed that the carbon contamination was evenly distributed throughout the catalyst structure. Other possible impurities such as calcium, phosphorus, sulphur, silicon, and chlorine remained below our XPS detection limits ($\approx 1\%$ of monolayer).

The pretreatment for the catalysts prior to TPD measurements was outgassing at 650 K in a vacuum of 1×10^{-10} Torr. Outgassing was stopped when no desorption of the residual gases was detected during a temperature ramp from 300 to 700 K, and the CO TPD profiles were fully reproducible. To avoid sintering of the Pd particles, the highest temperature employed in the TPD studies was 700 K.

All the gas exposures were performed using a molecular beam of CO or NO at a constant flux. CO (99.9%) and NO (99.9%) were supplied by AGA Ltd. (Finland) and were used without further purification. The sample was clamped to a pyrolytic boron nitride heater element (a Fisons XL-system) and heated by conduction. An N-type (Nicrosil/Nisil) thermocouple was positioned directly against the sample. The TPD profiles were measured as a function of temperature which was varied from 300 K to 700 K at a linear rate of 7 K/s.

To obtain more information on the adsorption and the surface intermediates over a Pd catalyst separate adsorption experiments of CO and NO on the catalyst surface were made by the FT–IR technique (Perkin-Elmer 1760 FT–IR spectrometer). The chamber (Environmental Chamber, Specac 19930) allowed heating of a sample and introduction of fixed amounts of different gas components separately.

In some experiments, called static experiments, the spectra were recorded at successive temperatures in the range from room temperature to 673 K using a standard collection software, whereas in others, called GC–IRexperiments, the spectra were recorded at constant temperature using a GC–IR software. The background spectra in static experiments were always measured after the sample evacuation at 573 K at room temperature, whereas in GC–IR experiments the background spectra were measured at 573 K after the sample evacuation. The spectra were measured for the range from 4000 to 600 cm^{-1} using a resolution of 4 cm^{-1}.

In the FT–IR studies the reaction gas was introduced into the chamber in different sequences and at different temperatures.

The static experiments were made by introducing CO or NO alone into the chamber at room temperature, after which the chamber was closed and the temperature was increased stepwise to 373, 423, 473, 573, and 673 K at which temperatures the spectra were measured.

The GC–IR measurements were made at 573 K. CO or NO was first introduced into the chamber at the reaction temperature and the gas was allowed to adsorb on the catalyst surface during the first 10 min. Then the second gas, NO or CO, was introduced into the chamber and this mixture was allowed to react for the next 10 min after which the chamber was evacuated.

In the case of a three-component mixture the second gas (NO or CO) and the third gas (air) were introduced into the chamber after 7 and 14 min from the introduction of the first gas. The spectra were recorded at 0.5 min intervals; each spectrum took 25 min. This procedure allowed the simultaneous performance of adsorption and reaction studies. The partial pressures of NO, CO, and air used in the experiments were 60, 90, and 180 mbar, respectively. NO was introduced into the chamber as a 10% NO/N_2 gas (600 mbar).

3. RESULTS AND DISCUSSION

3.1. CO Adsorption

Figures 1 and 2 show the TPD profiles of CO desorption from the Pd catalysts (solid curves). All the catalysts were exposed to 60 L (Langmuirs) of CO at 300 K prior to the TPD measurements by using a molecular beam. In general, all the CO TPD curves exhibit a single maximum accompanied by a shoulder at lower temperature. Figures 1a, 2a, and 2b also show the CO TPD profiles from the different washcoats (dashed curves) illustrating only a fairly weak interaction of CO with Al_2O_3, $LaAlO_3$, and La_2O_3–Al_2O_3.

This weak interaction was also seen in FT–IR studies. Adsorption of CO on the fresh alumina washcoat gave rise to weak absorption bands at 1590, 1562, and 1397 cm^{-1} in the temperature range of 473 to 573 K. The region between 1700 and 1200 cm^{-1} includes carbon–oxygen bands such as carbonates, formates, and bicarbonates on the Al_2O_3 surface (18). The bands at 1596 and 1380–1376 cm^{-1} are assigned to the asymmetric and symmetric O-C-O stretching vibrations of adsorbed formate ions (19, 20). The absorption bands on the annealed washcoats were quite similar to those obtained for the fresh alumina washcoat (1594, 1560, and 1385 cm^{-1}). The absorption band at 2253 cm^{-1} at higher temperatures was most probably caused by the interaction of CO with Al_2O_3. According to the literature (21–23) the bands in the range from 2300 to 2170 cm^{-1} are due to CO molecules adsorbed on the Al_2O_3 support. For example, Marchese *et al.* (21) have shown that a CO band at 2247 cm^{-1} is associated with molecules adsorbed at the most acidic cationic sites. Thus, we believe that in our case (Al_2O_3

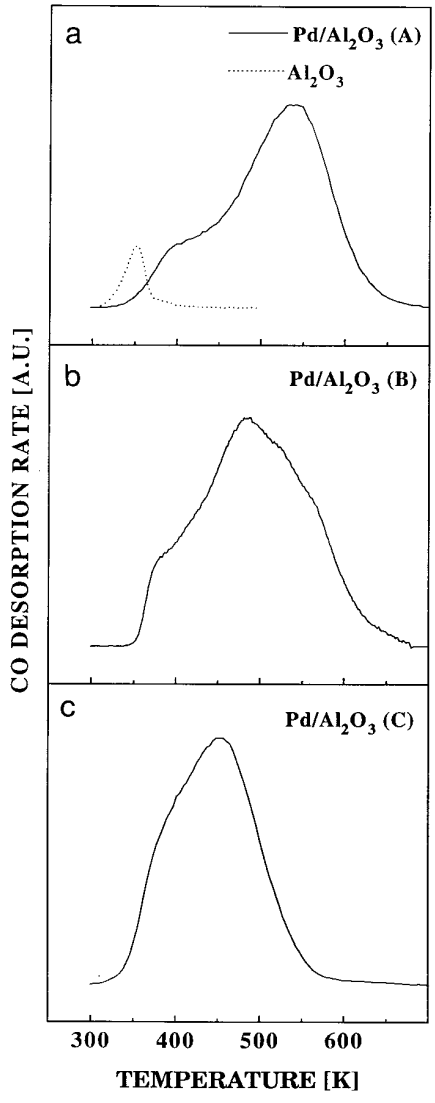

FIG. 1. Thermal desorption profiles for CO on Al_2O_3-supported Pd catalysts. Pd catalysts were exposed to 60 L (Langmuir) of CO at 300 K: (a) Pd/Al_2O_3 (A); (b) Pd/Al_2O_3 (B); (c) Pd/Al_2O_3 (C). The dashed curve in (a) is the TPD profile for Al_2O_3 washcoat. Heating rate 7 K/s.

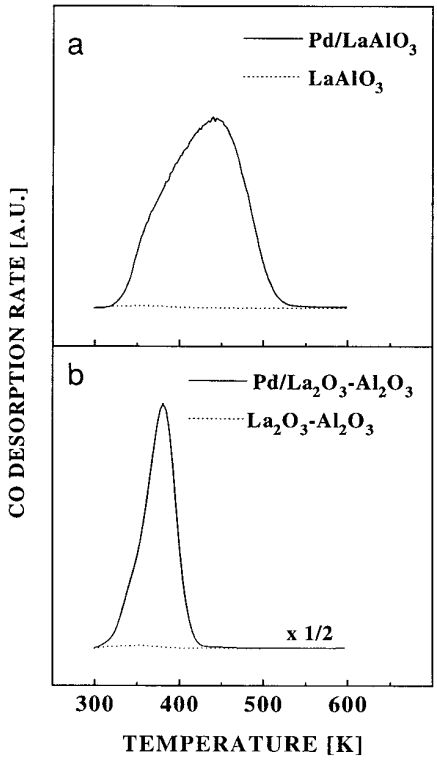

FIG. 2. Thermal desorption profiles for CO on La-modified Al_2O_3-supported Pd catalysts. Pd catalysts were exposed to 60 L of CO at 300 K: (a) $Pd/LaAlO_3$ and (b) Pd/La_2O_3–Al_2O_3. For both catalysts the chemical state of Pd was highly oxidized. The dashed curves are the TPD profiles for $LaAlO_3$ and La_2O_3–Al_2O_3 washcoats. Heating rate 7 K/s.

support mounted on a metal foil) the band at 2253 cm^{-1} represents CO σ-bonded to strong cationic Lewis acid sites that can be regarded as surface defects with strong Lewis acid character (24). The complexes that cause these bands can be denoted as Al^{3+}–CO (4). With IR very low concentrations of surface compounds can be detected under reaction conditions.

According to GC–IR studies the reaction of CO with the washcoat was much weaker at 473 K than at 573 K. A weak absorption band was observed at around 1590 cm^{-1} at lower temperature whereas at 573 K absorption bands at 1590, 1576 and around 1400 cm^{-1} were observed, indicating the formation of formate species. When the washcoat contained La_2O_3, the absorption bands at 1600–1200 cm^{-1} were weaker but the O-C-O stretching vibrations could be detected. The formate surface complex formation on the $LaAlO_3$ washcoat was extremely weak, indicating that the formation of formate species in this case was the least probable compared to the other two washcoat structures.

In Figs. 1 and 2 the position of the main desorption peak maximum is seen to shift from ~540 K on Pd/Al_2O_3 (A) (Fig. 1a) to ~375 K on Pd/La_2O_3–Al_2O_3 (Fig. 2b) indicating considerable changes in the CO bonding on these Pd catalysts. It is obvious that the CO binding energy strongly depends on the chemical and structural properties of the catalysts.

Based on the XPS results, the chemical state of palladium was found to be the most metallic on Pd/Al_2O_3 (A) (17). Therefore, a comparison between the CO TPD profile measured from Pd/Al_2O_3 (A) (Fig. 1a) and the profiles obtained from Pd single crystals and nonporous Pd model catalysts (25–43) is reasonable. The CO TPD curve in Fig. 1a bears a close resemblance to those observed from Pd(111) (28) and from large Pd particles (diameter >3 nm) supported on a nonporous alumina substrate (41). Therefore, it is suggested that the TPD results shown here are not strongly affected by porosity of the support or the carbon contamination.

Only fairly weak particle-size or crystallographic effects are expected to occur on the Pd catalysts. This is simply because the particle sizes in our catalysts are relatively large exhibiting a value greater than ~3.0 nm (ranging from 4.2 nm to 96 nm, Table 1) above which all the particle size effects usually observed in desorption kinetics approach the bulk-metal limit. In other words, for large Pd particles the CO TPD curves should resemble those of Pd(111) (28).

There are numerous studies reported in the literature of CO adsorption on Pd model catalysts (31–43). Most of these studies are quite controversial with respect to the dissociation of CO. Especially, the reactivity of small Pd particles in dissociation of CO has been an issue of debate between various research groups (40–43). The differences in support materials, washcoat compositions, and preparation conditions employed by different groups have been invoked to explain some of the existing discrepancies. At the moment, there exists no unambiguous explanation to rationalize the observed dissociation of CO on the Pd model catalysts.

The dissociation of CO was not observed on any of our Pd catalysts. Successive TPD runs of CO after adsorption of CO at room temperature were identical, and the concentration of the carbon impurity measured by XPS was about the same for all samples and remained constant during the experiments. It is suggested that one of the reasons for failing to observe the dissociation of CO is due to the relatively large particle sizes of the catalysts.

Stara and Matolin studied CO adsorption/dissociation on Pd/Al_2O_3 model catalysts (40). Using successive CO adsorption and desorption cycles to monitor the changes in the CO adsorption capacity due to carbon buildup, they found that the dissociation of CO was important only for Pd particles smaller than 2.5 nm. It has also been suggested that the CO disproportionation rate depends on the Pd particle size; the smaller the particle size, the higher the carbon formation rate (42). The Pd particle sizes of the catalysts used in this study range from 4.2 nm to 96 nm. Thus, it is not believed that the dissociation of CO was promoted by the crystallographic effects even with the smallest particle size of 4.2 nm.

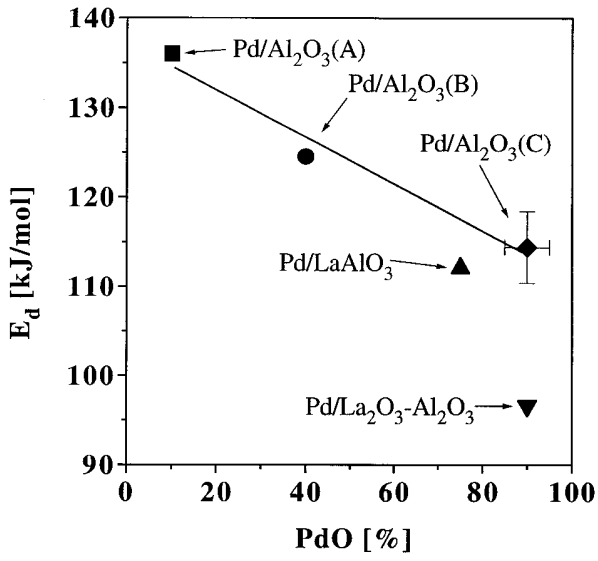

FIG. 3. CO activation energy of desorption as a function of the relative amount of PdO: Pd/Al_2O_3 (A) (■), Pd/Al_2O_3 (B) (●), Pd/Al_2O_3 (C) (◆), $Pd/LaAlO_3$ (△), and Pd/La_2O_3–Al_2O_3 (▽).

Another possible reason why the dissociation of CO was not observed can be related to the carbon atoms, some of which may have been adsorbed on those sites of the Pd particles which are probably the ones to dissociate CO, e.g., step sites (40). Hence, the dissociation of CO could be limited or even completely sterically blocked by these carbon atoms.

Since the dissociation of CO could not be seen within the detection limits of our measurements, it is concluded that none of the different washcoat compositions used in these studies, Al_2O_3, La_2O_3–Al_2O_3, and $LaAlO_3$, either directly or via the interaction with the Pd particles shows any considerable reactivity toward the dissociation of CO.

Clearly, the large shift of the main desorption peak maximum is the most pronounced effect seen by comparing the CO TPD curves with each other (Figs. 1 and 2). This shift can be attributed to remarkable differences in the CO bonding strength on these Pd catalysts. The activation energy of desorption E_d of CO for the main desorption peak for the five studied samples has been calculated using the first-order Redhead equation (44) assuming that the preexponential factor is of 10^{13} s^{-1}. These E_d's have been plotted in Fig. 3 against the amount of palladium oxide, noted as PdO, obtained from the XPS analysis (17). It turns out that E_d closely correlates with the chemical state of Pd.

Figure 3 also shows the results for the two La-modified Pd/Al_2O_3 catalysts, where the chemical state of palladium is highly oxidized. By comparing the CO TPD profile from Pd/Al_2O_3 (C) (Fig. 1c) with that of $Pd/LaAlO_3$ (Fig. 2a) one can see that the desorption peak maximum is slightly lower for $Pd/LaAlO_3$, but otherwise the two profiles are very similar. This similarity suggests that the presence of $LaAlO_3$ does not much alter the adsorption properties or the binding energy of CO on highly oxidized Pd particles.

In contrast to Pd catalysts supported on $LaAlO_3$ and Al_2O_3, the CO TPD profile of Pd/La_2O_3–Al_2O_3 (Fig. 2b) is dramatically different. The most striking feature in this profile is the very low binding energy of CO, as indicated in Fig. 3. The whole shape of the TPD curve is also very different and is characterized by the extremely narrow peak width. There seems to be a small shoulder at the low temperature side of the main peak. It is possible that some portion of the CO molecules already desorbs below the adsorption temperature used in these experiments (300 K) which can explain the narrow peak width. However, it is clear that the PdO–La_2O_3 interaction strongly destabilizes the bonding of CO.

Ladas *et al.* (45) studied the surface reactivity of high oxygen coverages on Pd single crystals where the penetration of chemisorbed oxygen into the bulk region of Pd can lead to the formation of subsurface oxygen species and eventually palladium oxide. Their results showed that the presence of a high coverage of oxygen substantially reduces the CO binding energy. It should be mentioned that the changes in CO bonding strength can greatly influence the reaction kinetics. For instance, the weakening of the CO bonding can have an inhibiting effect on the rate of CO_2 production for the catalytic CO–O_2 reaction, due to the lowering of CO residence time (46).

The surface complexes formed on Pd catalysts according to FT–IR analyses when CO alone was introduced into the cell were linear Pd^+–CO, which appeared at 2160 cm^{-1} already at room temperature, bridged Pd_x–CO at around 1990 cm^{-1} (weak bands) and Al^{3+}-CO complex at 573–673 K (2257–2253 cm^{-1}) (Fig. 4). The formation of carbonate species was observed at 1465–1457 cm^{-1}. The adsorption of CO on Pd catalysts depends greatly on the oxidation state of Pd (6). The most common bands are linear carbonyls at 2140–2100 cm^{-1} (Pd^+–CO), 2080–2000 cm^{-1} (Pd^0–CO) (7), strong multilaterally bonded carbonyls at 1965 and 1910 cm^{-1} (Pd_x–CO, bridged carbonyls at 2000–1800 cm^{-1}) (6, 8, 9) and triply bonded CO at 1880–1800 cm^{-1} (6). Absorption bands due to carbonate species appear normally at around 1638 and 1450 cm^{-1} (19). According to earlier studies (47), on a metallic Pd-catalyst prereduced with hydrogen strong bridged Pd_x–CO complex formation was observed at 1936 cm^{-1} and linear Pd^0–CO at 2065 cm^{-1}. Adsorption of CO on the washcoat as formate and carbonate gave absorption bands at 1588 and 1469 cm^{-1} (47).

With the fresh Pd/Al_2O_3 (B) sample the linear Pd^+–CO bands appeared at 2161 cm^{-1} (Fig. 4a). When the cell temperature was increased to 573 K the linear Pd^+–CO band disappeared and the formation of Al^{3+}–CO complex could be detected at 2257 cm^{-1}. When the sample was annealed and taken out of the oven at 773 K (Pd/Al_2O_3 (C))

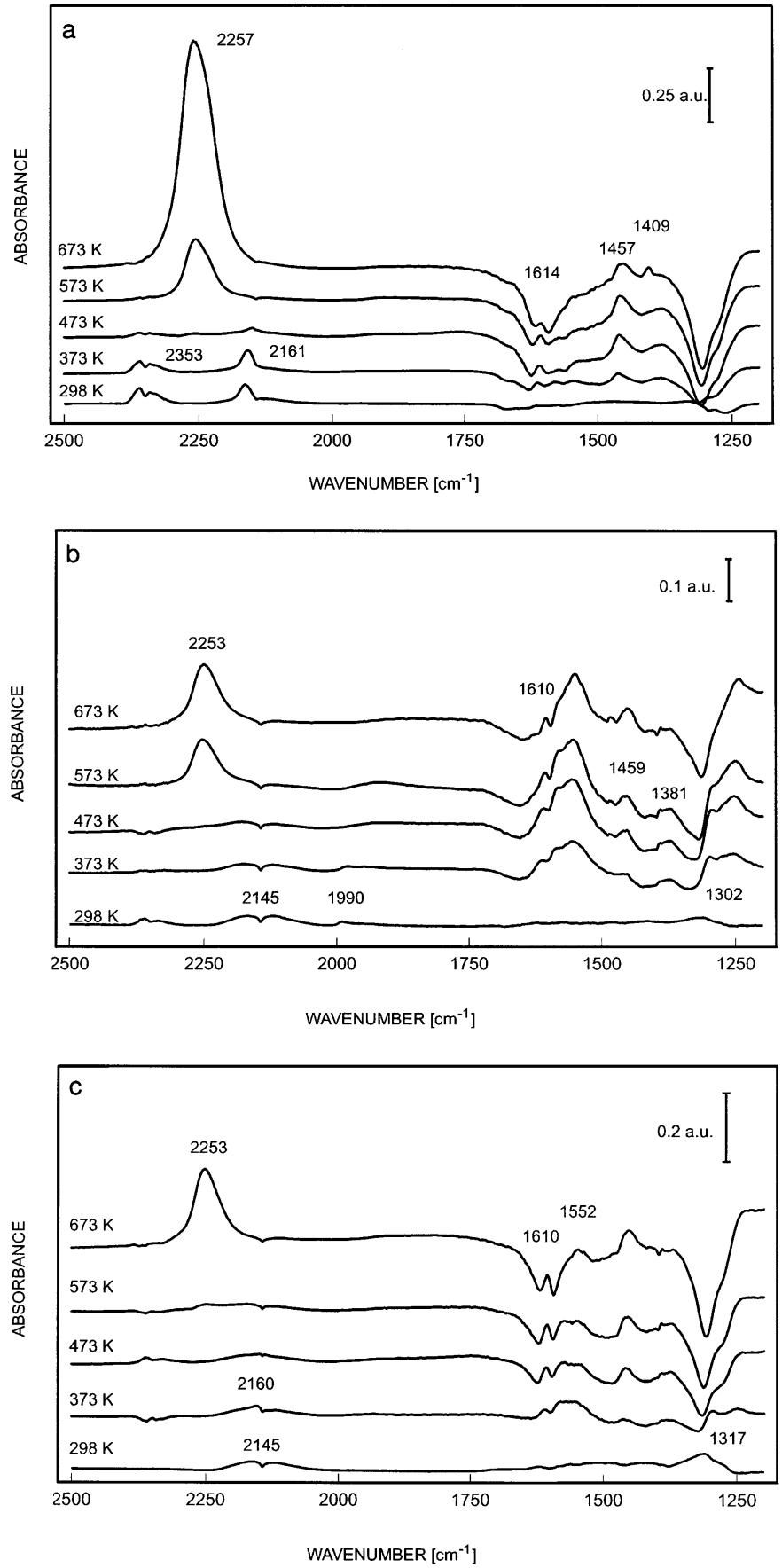

FIG. 4. CO adsorption on fresh and annealed Pd catalysts: (a) Pd/Al_2O_3 (B); (b) Pd/Al_2O_3 (C); (c) Pd/Al_2O_3 (A).

the absorption bands were weaker than those with the fresh Pd-catalyst (Fig. 4b). A weak absorption band at 1990 cm^{-1} is assigned to bridged Pd_x–CO complex formation. When the cell temperature was increased to 573–673 K the formation of Al^{3+}–CO complex started (2253 cm^{-1}). On the annealed Pd/Al_2O_3 catalyst which was taken out of the oven at 1223 K (Pd/Al_2O_3 (A)) the absorption bands were smooth. Only gaseous CO, Pd^{+}–CO, and Al^{3+}–CO complex formation were observed at 2145, 2160, and 2253 cm^{-1}, respectively. The interaction of CO with the alumina washcoat was similar to that with a fresh sample (Figs. 4a and 4b).

The contribution of the washcoat (Al_2O_3, La_2O_3–Al_2O_3, and $LaAlO_3$) to the adsorption and reaction of CO was evident. The reaction of CO with the washcoat stabilized by La to form carbonate species was the least probable with Pd/La_2O_3–Al_2O_3 and $Pd/LaAlO_3$.

3.2. NO Adsorption

Figures 5 and 6 show TPD profiles after 60 L exposure of NO at 300 K for the Pd catalysts. Along with the NO desorption there is a thermal reaction of NO with the catalysts during the TPD ramp, producing dinitrogen (N_2) and nitrous oxide (N_2O).

In sharp contrast to the case of CO, the interaction of NO with the washcoats, Al_2O_3, La_2O_3–Al_2O_3, and $LaAlO_3$, is significant. This is shown in Figs. 5a, 6a, and 6b (dashed curves). This interaction is also clearly observed in the FT–IR spectra. NO was adsorbed on the fresh and annealed Al_2O_3 already at room temperature, yielding the absorption bands at 1628, 1475, and 1232 cm^{-1} (Fig. 7a). These bands are proposed to originate from Al–NO_2 and Al–NO_3 species (4). At higher temperatures (373–573 K) the band intensities become even stronger. A band at 2249 cm^{-1} (373–673 K) is probably due to the presence of N_2O formed by NO dissociation (4). When the washcoat contained La_2O_3 besides alumina, the absorption bands at 1600–1200 cm^{-1} were weaker but the formation of nitrate and nitrite species could clearly be seen at 1624/1628, 1457, and 1270 cm^{-1}. The absorption bands at 1600–1200 cm^{-1} on the $LaAlO_3$ washcoat were very weak, indicating that the formation of nitrate and nitrite was the least probable when compared to the two other washcoat structures. The strongest band was observed at around 1270 cm^{-1} (NO_2^-, NO_3^-). Even though NO can molecularly adsorb on the supports, the absence of the N_2 TPD peak suggests that the Pd particles must be mainly responsible for the decomposition of NO.

Similarly as with CO the desorption peak maximum of NO is found to vary on different Pd catalysts changing from ~420 K on Pd/Al_2O_3 (A) to ~350 K on Pd/La_2O_3–Al_2O_3. This destabilization of NO adsorption increases as a function of the PdO as shown in Fig. 8. The activation energies of desorption have been calculated using the first-order Redhead equation assuming that the preexponential factor is 10^{13} s^{-1}. One can see from Fig. 8 that the higher the PdO concentration, the weaker the NO bonding, this being the most destabilized on Pd/La_2O_3–Al_2O_3. This behavior of NO is exactly the same as that of CO, although a change in E_d of NO when going from one catalyst to another is not as dramatic as with CO.

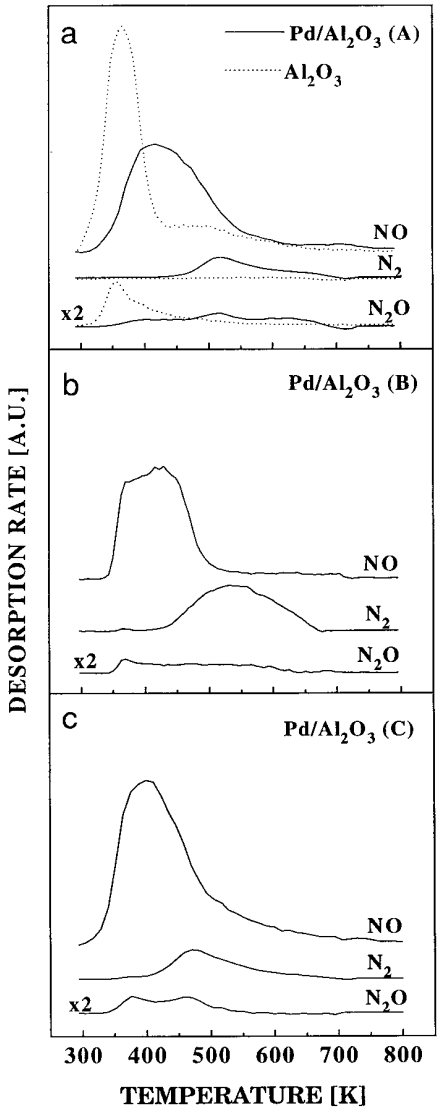

FIG. 5. Thermal desorption profiles for NO on Al_2O_3-supported Pd catalysts. Pd catalysts were exposed to 60 L of NO at 300 K: (a) Pd/Al_2O_3 (A); (b) Pd/Al_2O_3 (B); (c) Pd/Al_2O_3 (C). The dashed curves in (a) are the TPD profile for Al_2O_3 washcoat. Heating rate 7 K/s.

The NO TPD curves shown in Figs. 5 and 6 are quite different from those observed on Pd single crystals or Pd model catalysts. For instance, NO adsorbs molecularly on Pd(111) (28) and Pd(110) (48) and remains intact during the TPD ramp, whereas on a stepped Pd(l12) surface (Pd(S) [3(111) × (00l)]) (49) and on Al_2O_3- and SiO_2-supported

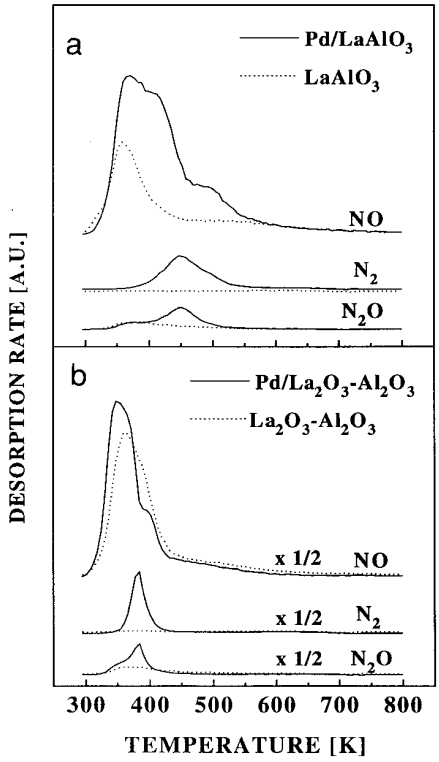

FIG. 6. Thermal desorption profiles for NO on La-modified Al_2O_3-supported Pd catalysts. Pd catalysts were exposed to 60 L of NO at 300 K: (a) $Pd/LaAlO_3$ and (b) Pd/La_2O_3–Al_2O_3. For both catalysts the chemical state of Pd was highly oxidized. The dashed curves are the TPD profiles for $LaAlO_3$ and La_2O_3–Al_2O_3 washcoats. Heating rate 7 K/s.

Pd model catalysts (41, 50) NO partially dissociates upon heating. Following the decomposition of NO the concomitant desorption of N_2 and N_2O is usually observed.

Ramsier *et al*. studied the effect of preadsorbed oxygen on the adsorption of NO on the stepped Pd(112) surface (51). They found that an increase in the amount of preadsorbed oxygen strongly weakens the NO adsorption bond, shifting the peak maximum from ~480 K to ~420 K. Simultaneously with the destabilization of NO the amount of N_2 and N_2O production decreases.

The TPD results of NO from the Al_2O_3-supported Pd catalysts in this study are consistent with those of Ramsier *et al*. (51) (see Fig. 5). However, the relative changes in the NO activation energies of desorption as well as the changes in relative yields of N_2 and N_2O (normalized to the total amount of adsorbed NO) are quite small, except for the fresh Pd/Al_2O_3 (Pd/Al_2O_3 (B)). The decrease in the NO activation energy of desorption is enhanced for the La-modified Pd/Al_2O_3 catalysts (Fig. 6b) but the relative amount of N_2 and N_2O formation stays at the same level as that for the Al_2O_3 supported Pd catalysts.

The adsorption and decomposition of NO on Pd single crystals and Pd model catalysts have been observed to be highly structure sensitive (28, 41, 48–51). For instance, Xu and Goodman (50) found that NO dissociation and reaction with CO on SiO_2-supported Pd model catalysts strongly depend on the metal particle size. Their results indicated that small Pd particles are more reactive than large particles in terms of the amount of NO dissociation (~50% for 3.0 nm particles and ~20% for 25.0 nm particles) but the small particles exhibit lower activities for N_2O formation. The same behavior was also seen on $A1_2O_3$-supported Pd model catalysts (41).

The results obtained in this study are in good agreement with the observations mentioned above for the Pd model catalysts as to the dissociation of NO. The relative amount of NO dissociation for the Pd/Al_2O_3 (A) and Pd/Al_2O_3 (C) catalysts is ~25%, the Pd particle sizes being 51 nm and 95 nm, respectively. For the fresh Pd/Al_2O_3 catalyst (Pd/Al_2O_3 (B)) the relative amount of NO dissociation is ~50%. This enhancement in dissociation can be interpreted as due to the smaller particle size (4.2 nm). The fact that some formation of N_2O is always seen during the temperature programmed desorption is consistent with the results obtained from the model catalysts and they can also be attributed to the effect of Pd particle size. However, no clear indication of a promotion of NO dissociation due to the presence of La_2O_3 or $LaAlO_3$ in the Pd catalysts was found.

Adsorption of NO on the fresh Pd/Al2O (Pd/Al_2O_3 (B)) yielded Pd^{2+}–NO already at room temperature. These absorption hands were observed at 1855 and 1815 cm^{-1}. NO forms linear surface complexes with Pd in the range of 1830–1650 cm^{-1} (Pd^{2+}–NO, Pd–NO^+, Pd–NO^-) (10–14). Weak linear Pd^+–NO bonding was observed at 1780 cm^{-1}. These linear bands disappeared at 473–673 K giving rise to nitrate and nitrite complex formation on alumina which was observed at 1600–1200 cm^{-1}. Typical absorption bands were observed at 1612, 1463, and 1240 cm^{-1}. The formation of an absorption band at l6l2 cm^{-1} is probably caused by NO_2. The infrared bands of adsorbed NO_2 are normally observed at 1618, 1318, and 750 cm^{-1} (52). Adsorbed NO_2 species can be formed when the gaseous NO reacts with oxygen bonded to Pd and created by the dissociation of NO. With a Pd-catalyst prereduced with hydrogen, strong bridged Pd_x–NO complex formation was observed at around 1800 cm^{-1}. Adsorption of NO on the annealed Pd/Al_2O_3 catalyst taken out of the oven at 773 K (Pd/Al_2O_3 (C)) gave linearly bonded Pd–NO already at room temperature (1715 cm^{-1}). This absorption band disappeared at 373 K. The linear Pd–NO bonding could not be seen at room temperature on a catalyst taken out of the oven at 1223 K (Fig. 7b). However, at 473–673 K traces of linear Pd^+–NO complex formation could be detected at 1780–1750 cm^{-1}. Typical absorption bands for adsorbed NO_2, nitrate or nitrite complex formation were observed at 1612 and 1461 cm^{-1}. At 573 to 673 K a strong absorption band at 2243 cm^{-1} was observed indicating the formation of N_2O.

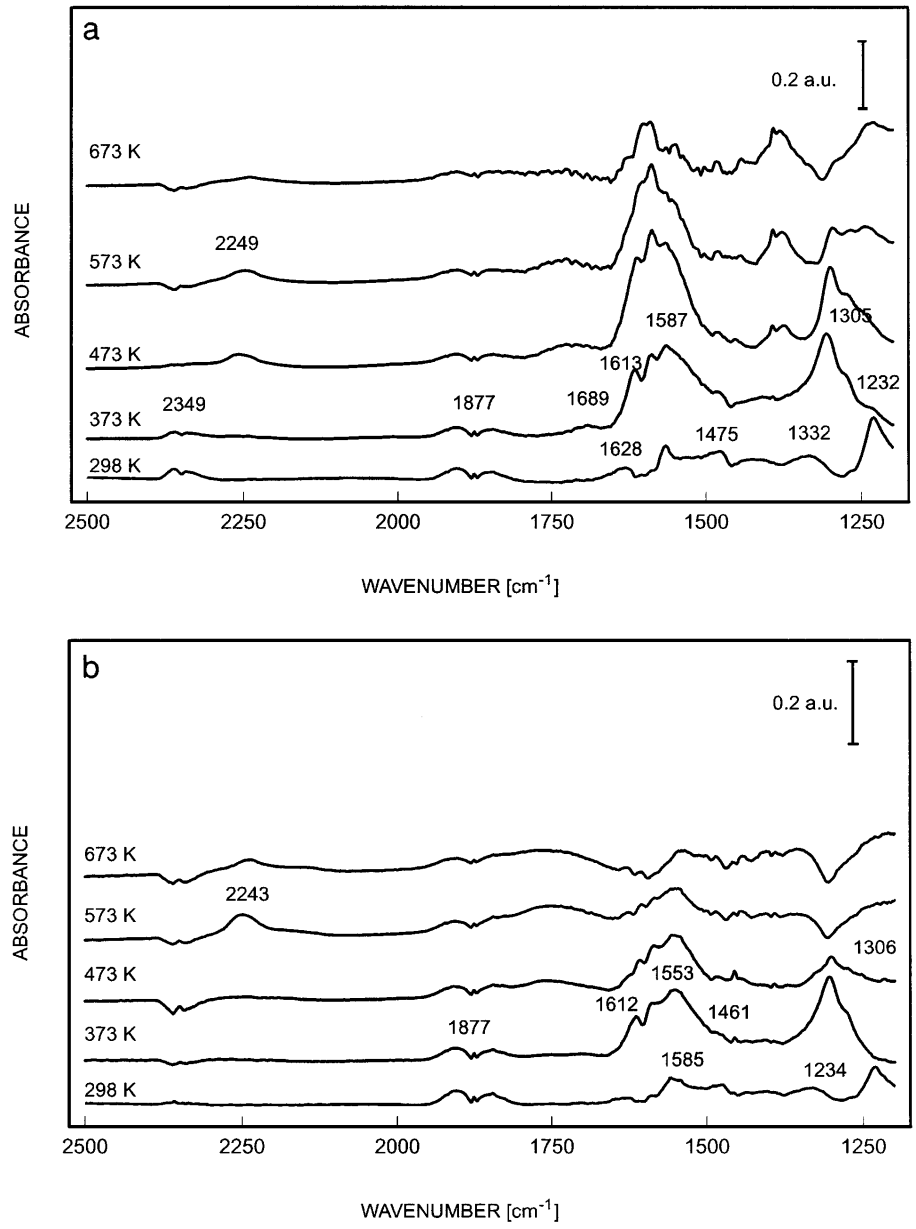

FIG. 7. NO adsorption on annealed (1223 K) alumina washcoat and Pd catalysts with different washcoat structures: (a) Al_2O_3, (b) Pd/Al_2O_3 (A); (c) Pd/La_2O_3–$A1_2O_3$; (d) $Pd/LaAlO_3$.

Adsorption of NO on Pd/La_2O_3–Al_2O_3 resulted in absorption bands at 1620, 1532, and 1290 cm^{-1}, due to the formation of adsorbed NO_2 and nitrate and/or nitrite species on the washcoat (Fig. 7c). The nitrate and nitrite formation was, however, much weaker than in the case of the alumina washcoat without lanthanum oxide. Traces of N_2O formation were observed at 573–673 K (weak absorption bands at around 2240 cm^{-1}). At 473–573 K NO formed linear Pd–NO complexes at 1770–1760 cm^{-1}. Adsorption of NO on $Pd/LaAlO_3$ indicated that the nitrate and nitrite formation on the washcoat at 1600–1200 cm^{-1} was much weaker than in the case of Al_2O_3 or La_2O_3–Al_2O_3 washcoats (Fig. 7d). This can be explained by the low BET surface area of the lanthanum aluminate support (5.9 m^2/g) compared to alumina (155 to 116 m^2/g) and lanthana-modified alumina (50 m^2/g) supports. No linear Pd–NO complex formation or N_2O formation could be detected.

Xu and Goodman (50) proposed that large Pd particles supported on SiO_2 provide two types of adsorption sites for NO: sites with a strong chemisorption bond for NO and other sites which dissociate NO. The N_2O formation was proposed to occur between molecularly adsorbed NO

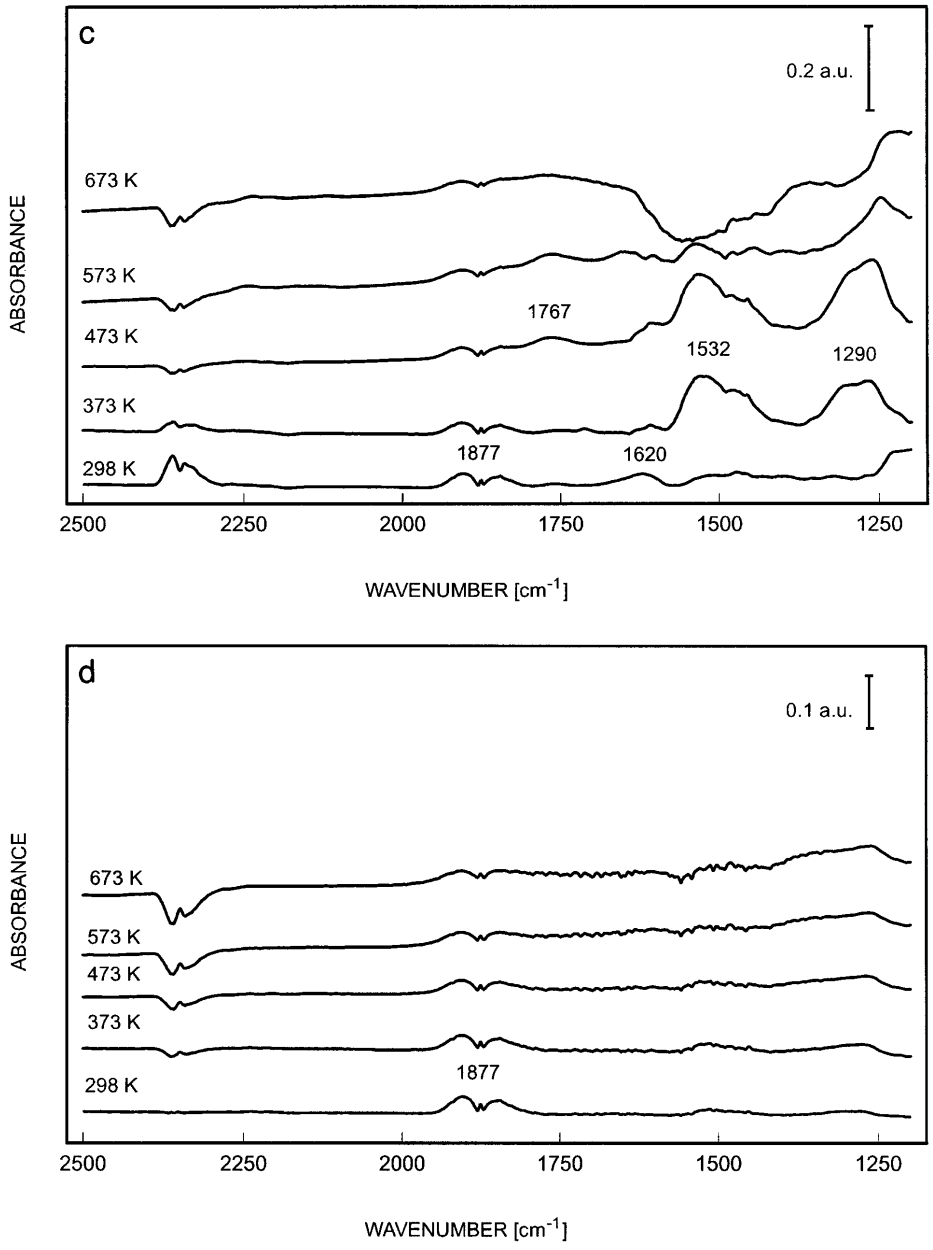

FIG. 7—*Continued*

and atomically adsorbed nitrogen (53). Hence. the reaction channel for N_2O formation on large Pd particles was interpreted as due to the presence of these adsorption sites which could simultaneously hold NO_{ads} and N_{ads} on the surface. Our TPD and FT–IR results support this mechanism for N_2O formation because the N_2O TPD peak appears just after the broad NO TPD peak maximum and in the FT–IR adsorption experiments an absorption band at 2249–2243 cm^{-1} is seen indicating the formation of N_2O. Therefore, it is likely that at the temperature where the N_2O formation rate reaches its maximum, there exist sufficiently high coverages of both NO_{ads} and N_{ads}.

4. CONCLUSIONS

The results in this study demonstrate that the effect of the chemical state of Pd in $Al_2O_3^-$, $LaAlO_3^-$, and La_2O_3–Al_2O_3-supported Pd catalysts for CO and NO adsorption and for the effects of temperature on their chemistry is significant.

TPD experiments reveal that the CO binding energy strongly decreases in the presence of PdO on the Al_2O_3-supported catalysts. For the La-modified catalysts in which palladium is in a highly oxidized state, the CO binding energy is even further reduced. According to the FT–IR exper-

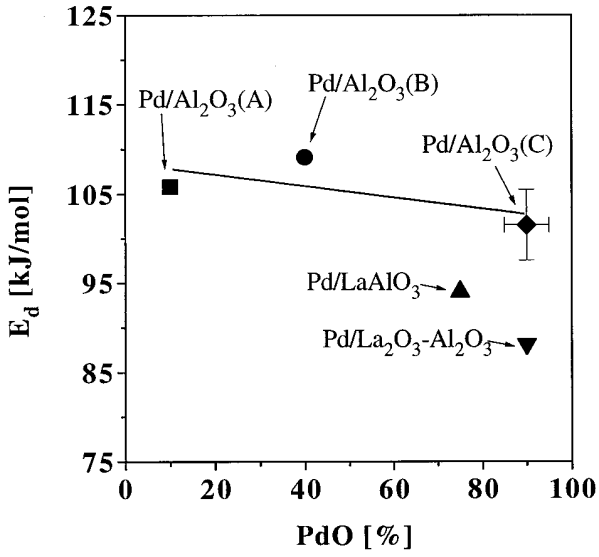

FIG. 8. NO activation energy of desorption as a function of the relative amount of PdO: Pd/Al_2O_3 (A) (■); Pd/Al_2O_3 (B) (●); Pd/Al_2O_3 (C) (◆); $Pd/LaAlO_3$ (△); Pd/La_2O_3–Al_2O_3 (▽).

iments, CO adsorption on the fresh $Pd/A1_2O_3$ (Pd/Al_2O_3 (B)) forms linearly bonded and bridged Pd–CO species. Adsorption of CO on the annealed samples gives rise to linearly bonded Pd–CO and Al^{3+}–CO complexes. CO also reacts with the alumina washcoat forming formate and carbonate species.

Similarly to the case of CO, the thermal stability of NO is decreased as the amount of PdO is increased for the Al_2O_3-supported catalysts. The reactivity of NO with the different Pd catalysts also appears to be related to the morphology of the adsorption sites. However, it seems likely that the observed strong interaction of NO with the supports can have important implications for the adsorption and decomposition of NO on Pd particles. Adsorption of NO on the fresh Pd/Al_2O_3 (Pd/Al_2O_3 (B)) gives linearly bonded Pd–NO already at room temperature. However, on the annealed samples only the linear Pd^+–NO complex formation can be detected. The NO_2 formation indicates the reaction of gaseous NO with oxygen atoms bonded to Pd and created by the dissociation of NO. The interaction of NO with the washcoat is strong, leading to nitrate and nitrite complex formation. At 573 to 673 K an absorption band at 2243 cm^{-1} is observed indicating the formation of N_2O. If the washcoat comprises lanthanum, the formation of nitrate, nitrite, formate, and carbonate species is weak.

ACKNOWLEDGMENTS

M. V., N. X., J. P., and J. A. wish to acknowledge Kemira Metalkat Oy, the Technology Development Center and the Academy of Finland for financial support.

REFERENCES

1. Summers, J. C., and Williamson, W. B., *ACS Symp. Ser.* **552**, 94 (1994).
2. Härkönen, M., Kivioja, M., Lappi, P., Mannila, P., Maunula, T., and Slotte, T., *SAE Tech. Pap. Ser.* **940935**, 303 (1994).
3. Subramanian, S., Kudla, R. J., Peters, C. R., and Chattha, M. S., *Catal. Lett.* **16**, 323 (1992).
4. Arai, H., and Tominaga, H., *J. Catal.* **43**, 131 (1976).
5. Marchese, L., Borello, E., Coluccia, S., Martra, G., and Zecchina, A., *in* "Proc. Int. Congr. Catal., 10th, Budapest 1992" (L. Guczi, F. Solymosi, and P. Tétényi, Eds.), p. 2523. Elsevier, Amsterdam, 1993.
6. Choi, K. I., and Vannice, M. A., *J. Catal.* **127**, 465 (1991).
7. Pitchon, V., Primet, M., and Praliaud, H., *Appl. Catal.* **62**, 317 (1990).
8. Duplan, J. L., and Praliaud, H., *Appl. Catal.* **67**, 325 (1991).
9. Burkett, H. D., Worley, S. D., and Dai, C. H., *Chem. Phys. Lett.* **173**(5/6), 430 (1990).
10. Unland, M. L., *J. Catal.* **31**, 459 (1973).
11. Hoyos, L. J., Primet, M., and Praliaud, H., *J. Chem. Soc. Faraday Trans.* **88**, 3367 (1992).
12. Mergler, Y. J., Ramsaransing, D. R. G., and Nieuwenhuys, B. E., in *Recueil,* accepted.
13. Alikina, G. M., Davidov, A. A., Sazonova, I. C., and Popovskii, V. V., *Kinet. Katal.* **28**, 418 (1987).
14. Grill, C. M., and Gonzalez, R. D., *J. Phys. Chem.* **84**, 878 (1980).
15. Valden, M., Licentiate thesis, Tampere University of Technology, Tampere, Finland, 1993.
16. Otto, K., Haack, L. P., and de Vries, J. E., *Appl. Catal. B* **1**, 1 (1992).
17. Maunula, T., Valden, M., Aaltonen, J., Xiang, N., Pere, J., Pessa, M., Savimäki, A., Lahti, A., and Härkönen, M., *J. Catal.* **161**, (2), (1996).
18. Haaland, D. M., and Williams, F. L., *J. Catal.* **76**, 450 (1982).
19. Erdöhelyi, A., Pásztor, M., and Solymosi, F., *J. Catal.* **98**, 166 (1986).
20. Solymosi, F., Erdöhelyi, A., and Lancz, M., *J. Catal.* **95**, 567 (1985).
21. Marchese, I., Boccuti, M. R., Coluccia, S., Lavagnino, S., Zecchina, A., Bonnevito, L., and Che, M., *in* "Structure and Reactivity of Surfaces" (C. Morterra, A. Zecchina, and G. Costa, Eds.), p. 653, Elsevier, Amsterdam, 1989.
22. Della Gatta, G., Fubini, B., Ghiotti, G., and Morterra, C., *J. Catal.* **43**, 90 (1976).
23. Tsyganenko, A. A., Denisenko, L. A., Zverev, S. M., and Filimonov, V. N., *J. Catal.* **94**, 10 (1985).
24. Zecchina, A., Escalona Platero, E., and Otero Areán, C., *J. Catal.* **107**, 244 (1987).
25. Engel, T., and Ertl, G., *Adv. Catal.* **28**, 1 (1979).
26. Conrad, H., Ertl, G., and Kuppers, J., *Surf. Sci.* **76**, 323 (1978).
27. Ratajczykowa, I., *Surf. Sci.* **152/153**, 627 (1985).
28. Kuhn, W. K., Szanyi, J., and Goodman, D. W., *Surf. Sci. Lett.* **274**, L611 (1992).
29. Szanyi, J., and Goodman, D. W., *J. Phys. Chem.* **98**, 2972 (1994).
30. Szanyi, J., Kuhn, W. K., and Goodman, D. W., *J. Phys. Chem.* **98**, 2978 (1994).
31. Gillet, E., Channakhone, S., and Matolin, V., *J. Catal.* **97**, 437 (1986).
32. Ladas, S., Poppa, H., and Boudart, M., *Surf. Sci.* **102**, 151 (1981).
33. Henry, C., *Surf. Sci.* **223**, 519 (1989).
34. El-Yakhloufi, M. H., and Gillet, E., *Catal. Lett.* **17**, 11 (1993).
35. Henry, C., Chapon, C., and Duriez, C., *J. Chem. Phys.* **95**, 700 (1991).
36. Matolin, V., Jungwirthova, I., and Tomkova, E., *Prog. Surf. Sci.* **35**, 175 (1991).
37. Ichikawa, S., Poppa, H., and Boudart, M., *J. Catal.* **91**, 1 (1985).
38. Corma, A., Martin, M., and Perez-Pariente, J., *Surf. Sci. Lett.* **136**, L31 (1984).
39. Xu, X., and Goodman, D. W., *J. Phys. Chem.* **97**, 7711 (1993).
40. Stara, I., and Matolin, V., *Surf. Sci.* **313**, 99 (1994).
41. Cordatos, H., Bunluesin, T., and Gorte, R. J., *Surf. Sci.* **323**, 219 (1995).

42. Matolin, V., and Gillet, E., *Surf. Sci.* **238**, 75 (1990).
43. Henry, C., Chapon, C., Goyhenex, C., and Monot, R., *Surf. Sci.* **272**, 283 (1992).
44. Redhead, P. A., *Vacuum* **12**, 203 (1962).
45. Ladas, S., Imbihl, R., and Ertl, G., *Surf. Sci.* **280**, 14 (1993) and references therein.
46. Ladas, S., Imbihl, R., and Ertl, G., *Surf. Sci.* **219**, 88 (1989).
47. Keiski, R. L., Härkönen, M., Lahti, A., Maunula, T., Savimäki, A., and Slotte, T., *in* "Proceedings, CAPoC3 Conference, Brussels, 1994," p. 53.
48. Raval, R., Harrison, M. A., Haq, S., and King, D. A., *Surf. Sci.* **294**, 10 (1993).
49. Ramsier, R. D., Lee, K.-W., and Yates Jr., J. T., *Surf. Sci.* **322**, 243 (1995).
50. Xu, X., and Goodman, D. W., *Catal. Lett.* **24**, 31 (1994).
51. Ramsier, R. D., Lee, K.-W., and Yates Jr., J. T. *Langmuir* **11**, 169 (1995).
52. Nakamoto, K., "Infrared Spectra of Inorganic and Coordination Compounds," Wiley, New York, 1970.
53. Cho, B. K., *J. Catal.* **138**, 255 (1992).